Mechanical Performance of Polylactic Acid from Sustainable Screw-Based 3D Printing

Mechanical Performance of Polylactic Acid from Sustainable Screw-Based 3D Printing

Paolo Minetola[1,3], Luca Fontana[1], Rossella Arrigo[2], Giulio Malucelli[2] and Luca Iuliano[1,3]

[1] Politecnico di Torino, Department of Management and Production Engineering (DIGEP), Corso Duca degli Abruzzi 24, 10129 Torino, Italy

[2] Politecnico di Torino, Department of Applied Science and Technology (DISAT), Corso Duca degli Abruzzi 24, 10129 Torino, Italy

[3] Politecnico di Torino, Integrated Additive Manufacturing Centre (IAM@PoliTO), Corso Duca degli Abruzzi 24, 10129 Torino, Italy

Please refer to the published version and cite this work as:

Minetola P., Fontana L., Arrigo R., Malucelli G., Iuliano L. (2021) Mechanical Performance of Polylactic Acid from Sustainable Screw-Based 3D Printing. In: Scholz S.G., Howlett R.J., Setchi R. (eds) Sustainable Design and Manufacturing 2020. Smart Innovation, Systems and Technologies, vol 200. Springer, Singapore. https://doi.org/10.1007/978-981-15-8131-1_47

On the mechanical performance of Polylactic Acid from sustainable screw-based 3D printing

Paolo Minetola[1,3] [0000-0002-5917-5273], Luca Fontana[1], Rossella Arrigo[2] [0000-0002-0291-2519], Giulio Malucelli[2] [0000-0002-0459-7698] and Luca Iuliano[1,3] [0000-0003-2029-8310]

[1] Politecnico di Torino, Department of Management and Production Engineering (DIGEP), Corso Duca degli Abruzzi 24, 10129 Torino, Italy
paolo.minetola@polito.it
luca.fontana@polito.it
luca.iuliano@polito.it

[2] Politecnico di Torino, Department of Applied Science and Technology (DISAT), Corso Duca degli Abruzzi 24, 10129 Torino, Italy
rossella.arrigo@polito.it
giulio.malucelli@polito.it

[3] Politecnico di Torino, Integrated Additive Manufacturing Centre (IAM@PoliTO), Corso Duca degli Abruzzi 24, 10129 Torino, Italy

Abstract. Screw-extrusion based 3D printing or Fused Granular Fabrication (FGF) is a less widespread variant of filament-based 3D printing for polymers. An FGF printer can be fed directly from polymer granules for improved sustainability. Shorter manufacturing routes and the potential of using recycled pellets from waste plastics are key features of FGF in the circular economy framework. A modified version of a standard Prusa i3 plus printer, which was equipped with a Mahor screw extruder, is used to test the mechanical performance of Polylactic Acid (PLA) processed with different layer infill and printing speed. Rheological and thermal analyses are carried out to characterize the material. The energy consumption of the FGF printer was measured during the fabrication of Dumbbell specimens. Tensile test results are consistent with other investigations presented in the literature. A higher printing speed promotes FGF eco-efficiency without a detrimental effect on the material strength, whereas lower printing speed should be preferred for increased material stiffness.

Keywords: 3D Printing, PLA, pellets.

1 Introduction

After the expiration of Stratasys key patent for Fused Deposition Modelling (FDM) technology in 2009, a wide number of low-cost 3D printers for Fused Filament Fabrication (FFF) has been developed and is available in the market. FDM and FFF processes are more popularly named as 3D printing and the feed-stock is a thermoplastic filament that is melted, extruded, and deposited over the print bed layer-wise [1].

Despite the wide diffusion and popularity of 3D printing that is favoured by a relatively low cost of materials and machine, the need to fabricate the semi-finished product of the polymeric filament introduces inefficiencies in the sustainability of 3D printed product life-cycle. Rather than using polymeric pellets for manufacturing the filament, the granules can be directly used as feedstock for 3D printing. This alternative involves the elimination of the filament production step throughout the manufacturing route of 3D printed products and enables easier recycling of 3D printing scraps [2]. Therefore the resources are exploited with more efficiency for the same goal of layered manufacturing. No energy is wasted in the filament fabrication step and the raw thermoplastic does not undergo partial processing that can adversely affect material properties because of the thermal cycles and phase transformations.

Moreover, filament manufacturing requires narrow dimensional tolerances to avoid issues of bucking, slippage or blocking of the material in the feeding system of the 3D printer [3]. The filament is winded onto spools for storage purposes and the first portion of it is subjected to higher mechanical stress because of the smaller winding radius around the spool support. As a consequence, especially for less ductile polymers, the last part of the filament that is unwound from the spool breaks into fragile pieces and cannot be used for 3D printing.

Another disadvantage of conventional 3D printing is the limited range of thermoplastic polymers that are commercially available as filament feedstock. From the economic point of view, 3D printed filaments are sold at a price that is five to ten times higher than that of raw plastic.

To overcome the aforementioned shortcomings, the use of 3D printers with a modified extrusion head, which can be fed with thermoplastic granules like in traditional injection moulding, has been proposed in the literature. Pellet Additive Manufacturing (PAM), Fused Pellet Manufacturing or Modelling (FPM), and Fused Granular Fabrication (FGF) are the names used to refer to the pellet-extrusion process for layered manufacturing. The advantages of FGF over FFF rely on the continuous automatic feed of the 3D printer with a broader range of thermoplastic granules that can be mixed in the extruder, reduced thermal degradation of the polymer during printing, and the opportunity to use plastic wastes within the circular economy perspective.

Among industrial AM systems, one of the few machines that can be fed with pellets is the Arburg Freeformer. However, in the Arburg Plastic Freeforming (APF) process the plasticating screw is used to prepare the molten material, whose droplet deposition in the layer is dosed through a piezoelectric nozzle [4].

Two types of FGF have been proposed and investigated in the literature. The first type employs a plunger-based system like a syringe. For example, Volpato et al. used a piston to extrude polypropylene (PP) granules that were molten in a heated reservoir [5]. Conversely, more researchers have developed or used a screw-based extrusion head for continuous feeding of the 3D printer.

Reddy et al. studied the influence of main FGF process parameters on the product strength and surface finish [6]. Valkenaers et al. designed a screw extrusion system and presented some results for polycaprolactone (PCL) with a 0.2 mm nozzle [7]. Tseng et al. designed and developed a temperature-controlled screw extruder for PEEK (polyether ether ketone) [8], while a similar system with the addition of an automatic feeder

was proposed by Whyman et al. [9]. Woern et al. investigated the potential to use recycled particles for four thermoplastics [10]. Similar research was conducted by Reich et al. for waste polycarbonate (PC) [11].

To further extend the application of the FGF technology to large part manufacturing, Liu et al. proposed an extrusion system with two stages to increase the machine capacity. A traditional plasticating unit for polymer extrusion is used in the first stage to feed a dosing extruder for printing in the second stage [12]. Nieto et al. demonstrated the use of a screw extruder for printing large ABS (acrylonitrile butadiene styrene) and PLA parts that were assembled to build toilets for the naval industry [13]. With the aid of a multiphysics modeling software, Wang et al. designed a screw-based extrusion system to be mounted on an industrial robot [14].

Byard et al. demonstrated the economic and environmental sustainability deriving from the use of FGF for large-scale products using Fab Labs as recycling centres for 3D printing waste [15].

In this paper, a modified version of a low-cost 3D printer is used for screw extrusion printing of PLA. The material viscosity is evaluated together with the thermal and mechanical properties for different layer infill and printing speeds. Finally, the energy consumption of the 3D printing system is measured for eco-efficiency considerations.

2 Materials and methods

A description of the test equipment and testing procedures is provided in this section. The rheological behavior of the PLA material was evaluated before printing to get the reference value of the viscosity to assess the capacity of the screw extruder. Differential scanning calorimetry (DSC) was used to determine the percentage of crystallinity and the thermal transitions of the 3D printed material, including the glass transition temperature (Tg), crystallization temperature (Tc), and melting temperature (Tm). Tensile tests were carried out to evaluate the mechanical behaviour of the PLA processed by FGF.

2.1 Viscosity of PLA material

The pellets of natural PLA material were supplied by Mahor XYZ company, together with the pellet extruder. The granules, which are not perfectly spherical, have an average size of about 3.30 mm. The PLA pellets are sold at 8.80 €/kg, which is about half of the price of 1 kg spool of cheap coloured PLA.

The rheological behaviour of the Mahor PLA material was assessed with an ARES (TA Instrument, USA) strain-controlled rheometer in parallel plate geometry (plate diameter: 25 mm). Frequency scans were carried out from 10^{-1} to 10^{2} rad/s at different temperatures, under nitrogen atmosphere. The strain amplitude was selected for each sample in order to fall in the linear viscoelastic region.

Figure 1 reports the trend of complex viscosity as a function of frequency for the studied material at different temperatures. At the lowest tested temperature, PLA exhibit a Newtonian plateau in the low-frequency range, followed by a shear-thinning

behavior (characterized by a sharp decrease of the viscosity as a function of frequency) at higher frequency values. As expected, the Newtonian behavior is progressively more pronounced as the temperature increases and covers the whole investigated frequency range at 260 °C. This behavior can be attributed to the enhanced dynamics of PLA macromolecules at high temperature, with consequent anticipation of the macromolecular chain relaxation.

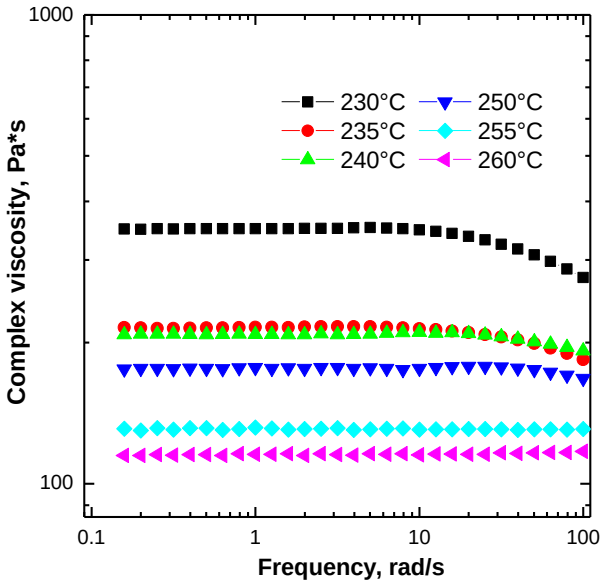

Fig. 1. Viscosity curves for PLA material

2.2 DSC analysis

DSC analyses were carried out using a QA1000 TA Instrument apparatus (Waters Lc, USA). All the experiments were performed under dry nitrogen gas (20 mL/min) using samples of around 8 mg in sealed aluminum pans. The PLA material was tested with a heating ramp from 0 to 200 °C at 10 °C/min.

2.3 Tensile tests

Tensile tests were carried out according to ASTM D638 guidelines (crosshead speed: 1 mm/min until 0.2% of deformation is reached and 10 mm/min up to sample break), using an Instron® 5966 dynamometer (Norwood, MA, USA). Dumbbell specimens of ASTM D638 type IV were 3D printed using different process parameters.

2.4 Screw-based 3D printer

A Prusa i3 Plus 3D printer was modified at Spazio Geco Fab Lab in Pavia (Italy) and equipped with a Mahor XYZ screw-based extruder for FGF technology and used for

the production of the tensile samples of PLA material. Apart from the extrusion head, the power supply was replaced with a 400W one to increase the heating capacity of the machine. The modified 3D printer can reach a maximum extrusion temperature of 290 °C and a maximum bed temperature of 90 °C. This way, the potential of the Prusa printer was extended to process a wider range of polymers from pellets.

The hopper of the extruder is a self-replicated part as in other modified 3D printers [16], whereas the nozzle has a diameter of 0.8 mm. The cartesian structure and axis resolution of the original machine remains unchanged. Thus, the FGF printer (Fig. 2) has a positioning accuracy of 0.004 mm for the Z axis and 0.012 mm for X and Y axes over a working volume of 300 x 300 x 420 mm.

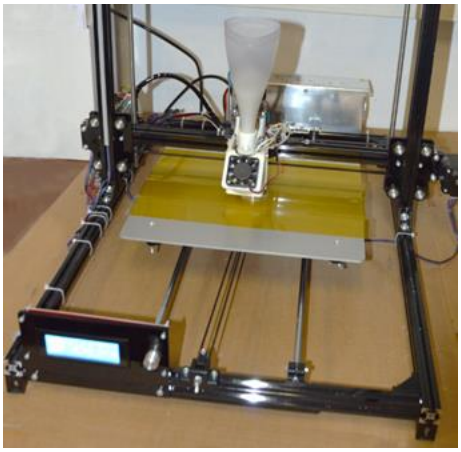

Fig. 2. Modified 3D printer with a Mahor extruder for FGF technology.

2.5 Slicing software

Slic3r open software was used to slice the STL (Solid To Layer) model of the object and generate the standard ISO .gcode file with the print path of each layer. Within the software, the configuration of the machine was replicated from the standard Prusa i3.

Nevertheless, before printing the PLA tensile sample, a hollow test cube was printed to calibrate the machine configuration and the printing parameters as suggested by Alexander et al. [2]. A Kapton ribbon tape (Fig. 2) was employed on the print bed to promote the adhesion of the first printing layer.

The test cube with an edge length of 20 mm and the thickness of 1 mm of the side walls was exploited for setting the optimal value of the parameter named extrusion multiplier. The extrusion multiplier setting is particularly critical in the change of the type of extrusion head, since this parameter allows the fine tuning of the extrusion flow rate, which in the Mahor head is defined by the rotation speed of the coaxial screw.

Figure 3 shows the replicas of the test cubes printed for different values of the extrusion multiplier. With the fixed set of parameters of Table 1, the optimal value of the extrusion multiplier was 0.6. Lower values decrease the flow rate and the mass of extruded and deposited material is insufficient. Conversely, for values of the extrusion

multiplier setting higher than 0.6, the sidewalls of the test cube become too thick because an excess of PLA material is extruded (Fig. 3).

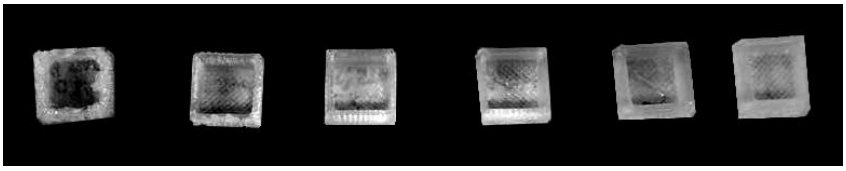

Fig. 3. Test cubes printed for different values of the extrusion multiplier.

Table 1. Main parameters used in Slic3r software for printing.

Parameter	Value
Layer height	0.3 mm
Extruder temperature	245 °C
First layer bed temperature	65 °C
Layer bed temperature	60 °C
Extrusion multiplier	0.6

Parameter	Value
Fill pattern	Rectilinear
Fill angle (referred to X axis)	-45° / +45°
Number of perimeters	1
Number of top solid layers	2
Number of bottom solid layers	2

3 Results

3.1 Specimen fabrication

A total of 18 Dumbbell specimens were fabricated with three levels of the infill of 25%, 50%, and 75% using the same parameters of the test cube (Table 1). The print path for the specimen in an intermediate layer is shown in Figure 4. Three replicas were produced for each infill percentage and each replica was 3D printed using two different speed sets for the extrusion head (Table 2).

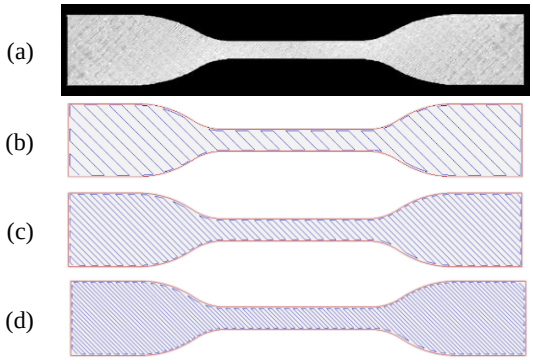

Fig. 4. Dumbbell specimen printed with 25% infill (a); print path for 25% infill (b); print path for 50% infill (c); print path for 75% infill (d).

Table 2. Speeds of the extrusion head in the two printing sets.

Parameter	High-speed printing set	Low-speed printing set
Perimeters	15 mm/s	7.5 mm/s
Infill (internal and top solid one)	15 mm/s	7.5 mm/s
Infill for solid and gaps	20 mm/s	10 mm/s
Bridges	30 mm/s	15 mm/s
Support material (skirt)	30 mm/s	15 mm/s
Speed for non-print moves	150 mm/s	100 mm/s
First layer speed	15 mm/s	7.5 mm/s

3.2 Specimen characteristics

After 3D printing, the thickness of each specimen was measured with a centesimal micrometer and the specimens were weighed using a Gibertini 1000HR-CM balance with a resolution of 0.01 g. The measures are reported in Table 3 along with the printing time and energy that was measured using a Meterk M34EU power meter plug.

Table 3. Measured characteristics of the tensile specimens.

Nr.	Infill (%)	Print speed (mm/s)	Thickness (mm)	Weight (g)	Average thickness (mm)	Average weight (g)	Printing time (min)	Energy (kWh)
1	75	15	4.10	4.961				
2	75	15	4.07	4.882	4.10	4.919	27	0.068
3	75	15	4.12	4.915				
4	75	7.5	4.11	4.899				
5	75	7.5	4.12	5.078	4.11	5.028	59	0.140
6	75	7.5	4.11	5.107				
8	50	15	4.14	4.112				
9	50	15	4.03	4.243	4.04	4.153	23	0.058
12	50	15	3.95	4.105				
7	50	7.5	4.19	4.072				
10	50	7.5	4.00	3.952	4.06	4.056	48	0.113
11	50	7.5	4.00	4.143				
16	25	15	3.98	3.305				
17	25	15	4.02	3.364	4.00	3.352	19	0.047
18	25	15	4.01	3.388				
13	25	7.5	3.93	3.316				
14	25	7.5	3.86	3.449	3.92	3.363	40	0.093
15	25	7.5	3.98	3.325				

3.3 Results of DSC analysis

The main thermal properties collected during the second heating scan are reported in Table 4. All the produced samples show reduced T_{cc} values as compared to unprocessed PLA, indicating an enhanced crystallization ability of PLA macro-molecules as a consequence of the 3D printing process.

The percentage of the crystalline phase is computed by equation 1.

$$X_c = \frac{\Delta H_m - \Delta H_{cc}}{\Delta H_m{}^0} \cdot 100 \quad (1)$$

where $\Delta H_m{}^0$ = 93 J/g.

As far as the content of the crystalline phase is concerned, unprocessed PLA is almost amorphous, while the processed samples show higher crystallinity degrees, due to the orientation experienced by PLA chains during processing, which promotes the formation of crystalline structures.

Table 4. Results of the DSC analysis.

	Tg (°C)	Tcc (°C)	Tm (°C)	ΔHcc (J/g)	ΔHm (J/g)	Xc (%)
Unprocessed PLA	62.9	112.4	177.8	27.1	30.8	3.98
PLA75%_15	63.9	101.7	178.4	34.9	57.5	24.3
PLA75%_7.5	64.2	100.7	178	37.9	58.3	21.9
PLA50%_15	65.0	104.2	179.7	37.4	51.0	14.6
PLA50%_7.5	64.9	102.7	179.3	38.3	52.5	15.3
PLA25%_15	64.6	106.7	178.9	31.9	47.0	16.2
PLA25%_7.5	64.6	104.3	179.2	36.7	50.2	14.5

3.4 Results of tensile testing

Table 5 collects the main mechanical properties, in terms of elastic module (E), ultimate tensile strength (UTS) and elongation at break, of all investigated samples.

Table 5. Results of the tensile test: average values and (*standard deviation*).

Specimen	E (MPa)	UTS (MPa)	Elongation at break (%)
PLA75%_15	782.76 (*135.04*)	23.03 (*1.53*)	4.54 (*0.48*)
PLA75%_7.5	1030.15 (*199.41*)	24.81 (*2.67*)	4.86 (*0.30*)
PLA50%_15	773.07 (*28.42*)	19.70 (*1.64*)	4.62 (*0.48*)
PLA50%_7.5	1079.26 (*269.21*)	18.86 (*1.71*)	4.22 (*0.18*)
PLA25%_15	763.05 (*208.44*)	19.03 (*0.67*)	4.34 (*0.36*)
PLA25%_7.5	1031.71 (*174.16*)	19.64 (*1.35*)	4.30 (*0.52*)

UTS and elongation at break are almost unaffected by the processing parameters, while higher elastic modulus values are observed for PLA samples processed with low printing speed.

4 Conclusions

In this paper, a screw extrusion FGF machine was used to test the performance of PLA material printed from pellet feedstock. The PLA granules were extruded at about 245 °C. Therefore, the Mahor extruder demonstrated good dosing capacity for a material viscosity of about 200 Pa·s (Fig. 1). This reference value, obtained by the rheological analysis of the PLA material, will be considered as a reference for future research activities involving the use of the same FGF printer with other thermoplastic pellets.

The results of the tensile tests for the printed PLA specimens, which were printed with different parameters, are consistent with previous results presented in the literature. When compared to the recent study of Wang et al. [17] for FFF printing, the higher layer thickness of the FGF specimens reduces the interlayer bonding strength.

The presence of air gaps increases as the infill percentage drops, so the higher UTS was obtained for the 75% infill with a beneficial effect of the higher crystallinity content, as evidenced by the DSC results. On the contrary, relevant differences in terms of UTS were not observed between the PLA specimens with 50% infill and those with 25% infill. The presence of two solid (100% infill) layers, on the top and bottom faces of the Dumbbell specimen for a total of 1.2 mm over the thickness of 4 mm, reduces the differences for lower percentages of the infill parameter.

Indications about an eco-efficient use of the modified FGF printer can be gathered by the comparison of the energy consumed for printing the different specimens to the actual strength obtained by tensile test results. As the value of UTS is not influenced by the printing speed, it is convenient to adopt higher printing speeds to complete the production in shorter times with related savings in terms of costs and energy. For every unit strength (MPa) of PLA material, about 0.01 MJ are consumed with the high-speed printing set of parameters, while around 0.02 MJ are necessary with the low-speed set. The highest eco-efficiency of 0.008 MJ/MPa is obtained in printing the specimen with 25% infill at 15 mm/s speed.

Further investigations are ongoing to identify the capacity of the modified screw-based 3D printer for processing other types of thermoplastics. Within the circular economy perspective, limitations of current screw design in printing recycled plastics should be investigated depending on the particle shape, size, and distribution. The opportunity to create blends by mixing different polymers or additives directly in the FGF extruder will be taken into consideration as well.

References

1. Calignano F., et al.: Overview on additive manufacturing technologies. 105(4), 593-612 (2017). doi: 10.1109/JPROC.2016.2625098.

2. Alexandre A., Cruz Sanchez F. A., Boudaoud H., Camargo M., Pearce J. M.: Mechanical Properties of Direct Waste Printing of Polylactic Acid with Universal Pellets Extruder: Comparison to Fused Filament Fabrication on Open-Source Desktop Three-Dimensional Printers. 3D Print. Addit. Manuf., (2020). doi: 10.1089/3dp.2019.0195.
3. Valkenaers H., Vogeler F., Voet A., Kruth J.-P.: Screw extrusion based 3D printing, a novel additive manufacturing technology. In: International Conference on Competitive Manufacturing, Stellenbosch, South Africa (2013).
4. Minetola P., Calignano F., Galati M.: Comparing geometric tolerance capabilities of additive manufacturing systems for polymers. Addit. Manuf. 32, 101103 (2020). doi: 10.1016/j.addma.2020.101103.
5. Volpato N., Kretschek D., Foggiatto J., da Silva Cruz C. G.: Experimental analysis of an extrusion system for additive manufacturing based on polymer pellets. Int. J. Adv. Manuf. Technol. 81(9-12), 1519-1531 (2015). doi: 10.1007/s00170-015-7300-2.
6. Reddy B., Reddy N., Ghosh A.: Fused deposition modelling using direct extrusion. Virtual Phys Prototyp 2(1), 51-60 (2007). doi: 10.1080/17452750701336486.
7. Valkenaers H., Vogeler F., Ferraris E., Voet A., Kruth J.-P.: A novel approach to additive manufacturing: screw extrusion 3D-printing. In: Proceedings of the 10th International Conference on Multi-Material Micro Manufacture, pp. 235-238. (2013).
8. Tseng J.-W., Liu C.-Y., Yen Y.-K., Belkner J., Bremicker T., Liu B. H., Sun T.-J., Wang A.-B.: Screw extrusion-based additive manufacturing of PEEK. Mater. Des. 140, 209-221 (2018). doi: 10.1016/j.matdes.2017.11.032.
9. Whyman S., Arif K. M., Potgieter J.: Design and development of an extrusion system for 3D printing biopolymer pellets. Int. J. Adv. Manuf. Technol. 96(9-12), 3417-3428 (2018). doi: 10.1007/s00170-018-1843-y.
10. Woern A. L., Byard D. J., Oakley R. B., Fiedler M. J., Snabes S. L., Pearce J. M.: Fused particle fabrication 3-D printing: Recycled materials' optimization and mechanical properties. 11(8), 1413 (2018). doi: 10.3390/ma11081413.
11. Reich M. J., Woern A. L., Tanikella N. G., Pearce J. M.: Mechanical properties and applications of recycled polycarbonate particle material extrusion-based additive manufacturing. 12(10), 1642 (2019). doi: 10.3390/ma12101642.
12. Liu X., Chi B., Jiao Z., Tan J., Liu F., Yang W.: A large-scale double-stage-screw 3 D printer for fused deposition of plastic pellets. J. Appl. Polym. Sci. 134(31), 45147 (2017). doi: 10.1002/app.45147.
13. Nieto D. M., López V. C., Molina S. I.: Large-format polymeric pellet-based additive manufacturing for the naval industry. Addit. Manuf. 23, 79-85 (2018). doi: 10.1016/j.addma.2018.07.012.
14. Wang Z., Liu R., Sparks T., Liou F.: Large-scale deposition system by an industrial robot (I): design of fused pellet modeling system and extrusion process analysis. 3D Print. Addit. Manuf. 3(1), 39-47 (2016). doi: 10.1089/3dp.2015.0029.
15. Byard D. J., Woern A. L., Oakley R. B., Fiedler M. J., Snabes S. L., Pearce J. M.: Green fab lab applications of large-area waste polymer-based additive manufacturing. Addit. Manuf. 27, 515-525 (2019). doi: 10.1016/j.addma.2019.03.006.
16. Minetola P., Galati M.: A challenge for enhancing the dimensional accuracy of a low-cost 3D printer by means of self-replicated parts. Addit. Manuf. 22, 256-264 (2018). doi: 10.1016/j.addma.2018.05.028.
17. Wang S., Ma Y., Deng Z., Zhang S., Cai J.: Effects of fused deposition modeling process parameters on tensile, dynamic mechanical properties of 3D printed polylactic acid materials. Polym. Test. 86, 106483 (2020). doi: 10.1016/j.polymertesting.2020.106483.